# Exosomes Secreted under Hypoxia Enhance Invasiveness and Stemness of Prostate Cancer Cells by Targeting Adherens Junction Molecules

**Anand Ramteke**[1,2], **Harold Ting**[1], **Chapla Agarwal**[1,3], **Samiha Mateen**[1], **Ranganathan Somasagara**[1], **Anowar Hussain**[2], **Michael Graner**[4], **Barbara Frederick**[3,5], **Rajesh Agarwal**[1,3], and **Gagan Deep**[1,3,*]

[1]Department of Pharmaceutical Sciences, Skaggs School of Pharmacy and Pharmaceutical Sciences, University of Colorado Denver

[2]Department of Molecular Biology and Biotechnology, Tezpur University, Tezpur, India

[3]University of Colorado Cancer Center, Aurora, Colorado

[4]Department of Neurosurgery, University of Colorado Denver, Aurora, Colorado

[5]Department of Radiation Oncology Anschutz Medical Campus, Aurora, Colorado

## Abstract

Hypoxic conditions in prostate cancer (PCA) are associated with poor prognosis; however, precise mechanism/s through which hypoxia promotes malignant phenotype remains unclear. Here, we analyzed the role of exosomes from hypoxic PCA cells in enhancing the invasiveness and stemness of naïve PCA cells, as well as in promoting cancer-associated fibroblast (CAF) phenotype in prostate stromal cells (PrSC). Human PCA LNCaP and PC3 cells were exposed to hypoxic (1% $O_2$) or normoxic (21% $O_2$) conditions, and exosomes secreted under hypoxic ($Exo^{Hypoxic}$) and normoxic ($Exo^{Normoxic}$) conditions were isolated from conditioned media. Nanoparticle tracking analysis revealed that $Exo^{Hypoxic}$ have smaller average size as compared to $Exo^{Normoxic}$. Immunoblotting results showed a higher level of tetraspanins (CD63 and CD81), heat shock proteins (HSP90 and HSP70) and Annexin II in $Exo^{Hypoxic}$ compared to $Exo^{Normoxic}$. Co-culturing with $Exo^{Hypoxic}$ increased the invasiveness and motility of naïve LNCaP and PC3 cells, respectively. $Exo^{Hypoxic}$ also promoted prostasphere formation by both LNCaP and PC3 cells, and enhanced α-SMA (a CAF biomarker) expression in PrSC. Compared to $Exo^{Normoxic}$, $Exo^{Hypoxic}$ showed higher metalloproteinases activity and increased level of diverse signaling molecules (TGF-β2, TNF1α, IL6, TSG101, Akt, ILK1, and β-catenin). Furthermore, proteome analysis revealed a higher number of proteins in $Exo^{Hypoxic}$ (160 proteins) compared to $Exo^{Normoxic}$ (62 proteins), primarily associated with the remodeling of epithelial adherens junction pathway. Importantly, $Exo^{Hypoxic}$ targeted the expression of adherens junction proteins in naïve PC3 cells. These findings suggest that $Exo^{Hypoxic}$ are loaded with unique proteins that could enhance invasiveness, stemness and induce microenvironment changes; thereby, promoting PCA aggressiveness.

*Corresponding Author: Gagan Deep, University of Colorado Denver, 12850 E. Montview Blvd, C238, Aurora, CO 80045. Phone: (303) 724-5553, Fax: (303) 724-7266, Gagan.deep@ucdenver.edu.

**Keywords**

Exosomes; Hypoxia; Invasiveness; Adheren junction; Prostate cancer

## INTRODUCTION

Prostate cancer (PCA) is the most common non-cutaneous malignancy and second leading cause of cancer-related deaths in American men. According to the American Cancer Society, in 2013, there will be an estimated 238,590 new cases and 29,720 deaths from PCA in the United States [1]. Patients with localized PCA have a high 5-year survival rate and a relatively low mortality to incidence ratio compared to other cancer types [2]. However, in patients with clinically detectable metastasis, median survival is reduced to only 12–15 months; therefore, metastasis is the main cause of high mortality among PCA patients [2–4]. Thus, a better understanding and targeting of the events associated with PCA growth and metastasis is warranted to lower mortality as well as to improve patient's quality of life.

Now it is clearly evident that the interaction between the tumor microenvironment and cancer cells plays a critical role in tumor growth, angiogenesis, epithelial to mesenchymal transition (EMT) and metastasis [5,6]. The tumor microenvironment consists of several distinct cell types, including tumor cells, cancer-associated fibroblasts (CAF), endothelial cells, macrophages, adipocytes, dendritic cells, natural killer cells, lymphocytes etc. In addition, the tumor microenvironment is rich in non-cellular components such as cytokines, growth factors, hormones and extracellular matrix. Tumor cells and microenvironment components communicate by cell-cell interaction as well as paracrine mechanisms involving growth factors, chemokines and proteinases [5,7]. Recently, exosomes and microvesicles have been suggested as one of the key mechanisms of intercellular communication in the tumor microenvironment [8,9]. Exosomes are approximately 30–100 nm diameter membrane-enclosed vesicles derived from the endosomal system during multivesicular body formation [10]. The factors and stimuli that regulate exosomes packaging and release have not been fully characterized, although exosomes have been widely reported to mediate local and systemic cell communication through horizontal transfer of information such as microRNAs, mRNAs and proteins [8,11,12]. In carcinogenesis, exosomes' role has been implicated in proliferation, angiogenesis, immune-suppression; and more recently, in the preparation of pre-metastatic niches in secondary organs [8,9]. For example, Peinado et al [13] recently reported that exosomes from highly metastatic melanomas increase metastasis by educating the bone marrow-derived cells at distant pre-metastatic sites. Interestingly, this study also showed that primary tumor growth as well as metastasis of melanoma cells could be compromised by inhibiting exosomes biogenesis [13]. Therefore, it is clear that a better understanding of the contents of exosomes and the conditions affecting their release as well as the microenvironment changes induced by exosomes could be useful towards targeting both primary tumor growth and metastasis.

Hypoxia (low oxygen conditions) in prostate tumors has been associated with an aggressive phenotype and poor prognosis [14,15]. Hypoxia is known to induce genetic and proteomic changes in cancer cells and to select clones with enhanced invasiveness, drug resistance and

stemness [15–17]. However, the mechanism/s underlying hypoxia-mediated increase of metastasis remains unclear; this is because hypoxic conditions mostly prevail away from the invasive front, which is usually at the tumor margins. In the present study, we assessed whether under hypoxic conditions PCA cells could enhance the invasiveness and motility of naïve PCA cells via transferring information packaged in exosomes. We characterized hypoxic PCA exosomes and analyzed their role in the motility, invasiveness and stemness of PCA cells. In addition, we analyzed the effect of exosomes on α-smooth muscle actin (α-SMA) expression in prostate fibroblasts. α-SMA is an established biomarker for the cancer-associated fibroblast (CAF) phenotype, which has been associated with the promotion of EMT, stemness and angiogenesis in PCA [18,19]. Furthermore, we identified the unique set of proteins that are loaded in hypoxic PCA exosomes and could be responsible for the enhanced invasiveness, stemness and microenvironment changes in PCA cells.

## MATERIAL AND METHODS

### Cell lines and reagents

Human PCA LNCaP and PC3 cells were purchased from ATCC (Manassas, VA). Human prostate stromal cells (PrSC), stromal cell growth medium (SCGM), and Bullet-kits were purchased from Lonza (Allendale, NJ). ExoQuick™, exosome-free FBS (Exo-FBS™) as well as antibodies for CD81, CD63, HSP70 and HSP90 were from System Biosciences (Mountain View, CA). Antibodies for TSG101, IL6, α-tubulin and α-SMA were from Abcam (Cambridge, MA). TGF-β2 antibody was from Gibco (Grand Island, NY). Antibodies for TNF1α, Annexin II, β-catenin and α-tubulin were from Santa Cruz Biotechnology (Santa Cruz, CA), and antibodies for E-cadherin, PKM2 (pyruvate kinase M2) and anti-rabbit peroxidase-conjugated secondary antibody were from Cell Signaling (Beverly, MA). DAPI was obtained from Sigma (St. Louis, MO). ECL (Enhanced Chemiluminescence) detection system and anti-mouse HRP-conjugated secondary antibody were from GE Healthcare (Buckinghamshire, UK). RPMI1640 medium and other cell culture materials were from Invitrogen Corporation (Gaithersburg, MD). AccQ Tag Fluor Reagent (WAT 052880), AccQ Taq Eluent A Concentrate (WAT 052890) and AccQ Tag HPLC Column (WAT 052885) were purchased from Waters Corporation (Milford, MA). All other reagents were obtained in their commercially available highest purity grade.

### Cell culture and hypoxia exposure

LNCaP and PC3 cells were cultured at 37°C in a 5% $CO_2$ humidified environment as adherent monolayer in RPMI1640 medium supplemented with 10% fetal bovine serum (FBS) or 10% heat inactivated FBS and 100 U/ml penicillin G and 100 μg/ml streptomycin sulfate. PrSC were cultured in SCGM supplemented with Bullet-kits. For exosome isolation, LNCaP and PC3 cells were cultured in media supplemented with exosome-depleted FBS. Hypoxia experiments were performed with a Hypoxia chamber (Coy Laboratory Products, Grass Lake, Michigan) at 1% $O_2$ at 37°C in a 5% $CO_2$ humidified environment.

### Exosome isolation

Exosomes were isolated from the conditioned media following a published method [11]. LNCaP and PC3 cells were cultured for 48 hrs; thereafter, media was replaced with RPMI

1640 supplemented with 10% exosome-depleted FBS and cultured under normoxic (21% $O_2$) or hypoxic (1% $O_2$) conditions for 72 hrs. Subsequently, conditioned media was harvested and exosomes were isolated by traditional methods using serial centrifugation at low speed, followed by ultracentrifugation (L-80 Ultracentrifuge, Beckman Coulter) at 30,000 rpm using type 70.1 Ti fixed angel rotor (Beckman Coulter). The exosomes were also isolated by a precipitation method using commercially available Exoquick™ reagent (System Biosciences) according to the vendor's instructions. Briefly, conditioned media was overnight incubated with Exoquick™ reagent, centrifuged at 5000 rpm for 2 hrs and the pellet was washed once with PBS, and pelleted exosomes were resuspended in PBS and stored at −20°C until further use.

### Nanoparticle tracking analysis (NTA)

Isolated exosomes were analyzed using Nanosight LM10 system (Nanosight Ltd, Navato, CA) equipped with a blue laser (405 nm). Nanoparticles were illuminated by the laser and their movement under Brownian motion was captured for 60 seconds and the video recorded was subjected to NTA using the Nanosight particle tracking software to calculate nanoparticle concentrations and size distribution.

### Electron microscopy

Exosomes were suspended in glutaraldehyde, and ~3–5 μl of exosomes were applied to 400 mesh copper grids (formvar/carbon coated, glow-discharged) for 5 minutes, followed by negative staining with 2% uranyl acetate for 2 minutes. Grids were briefly washed in DI water, allowed to dry and viewed using FEI Technai Transmission electron microscope equipped with Gatan Ultrascan digital high-resolution camera.

### Invasion assay

Invasion assay was performed using matrigel coated trans-well chambers from BD Biosciences (San Jose, CA). In this assay, bottom chambers were filled with RPMI medium with 10% FBS. LNCaP cells ($1 \times 10^5$) were incubated with 10 μg of LNCaP Exo$^{Normoxic}$ or Exo$^{Hypoxic}$ for 45 minutes in RPMI medium (with 0.5% FBS) and thereafter, seeded in the upper chambers. After 24 hrs of incubation under standard culture conditions, LNCaP cells on top surfaces of the membrane (non-invasive cells) were scraped with cotton swabs and cells on the bottom sides of the membrane (invasive cells) were fixed with cold methanol, stained with hematoxylin/eosin and mounted. Images were taken using Cannon Power Shot A640 camera on Zeiss inverted microscope and invasive cells were counted at 100×.

### Wound healing assay

The effect of LNCaP Exo$^{Normoxic}$ or Exo$^{Hypoxic}$ on the motility of PC3 cells was examined in well-established wound healing assay [20]. Briefly, PC3 cells were grown to full confluency in six-well plates and wounded by pipette tips and washed twice with media to remove detached cells. Photomicrographs of initial wounds were taken using Canon Power Shot A640 digital camera (at 100× magnification). Thereafter, cells were incubated with LNCaP Exo$^{Normoxic}$ or Exo$^{Hypoxic}$ (20 μg each). Experiment was terminated after 6 hrs and photomicrographs of final wounds were taken for each group. Initial and final wound sizes

were measured using AxioVision Rel.4.7 software, and difference between the two was used to determine migration distance using the formula: Initial wound size minus final wound size divided by 2.

### Prostasphere formation

Naïve LNCaP and PC3 cells ($2.5 \times 10^3$ cells per well) were separately cultured in Corning ultra-low attachment plates in DMEM/F-12(Ham) medium containing supplements B27 and N2 (from Invitrogen) in the presence of Exo$^{Normoxic}$ or Exo$^{Hypoxic}$ (10 μg/day each for 3–4 days) from LNCaP and PC3 cells, respectively. Number of prostaspheres formed was counted under a microscope after 5–6 days.

### Confocal imaging

PrSC were seeded onto glass coverslips in 12-well plates and incubated for 24 hrs in low serum (0.5%) growth media along with 20 μg of Exo$^{Normoxic}$ or Exo$^{Hypoxic}$ from LNCaP and PC3 cells. After the treatment, media was removed and cells were fixed with formaldehyde/cold methanol and incubated overnight in primary antibody (anti α-SMA). The cells were then washed and treated with secondary Alexa-Fluor 488 conjugated antibody and DAPI nuclear stain. The coverslips containing cells were then mounted onto slides and images were taken by Nikon Confocal Microscope. Images were quantified for Alexa-Fluor 488 -green color based upon the following scoring criterion: 0+ (no color), 1+ (dim color), 2+ (moderate color), 3+ (bright color), 4+ (very bright color).

### Zymogram analyses

MMP activity was determined by Zymogram assay following vendor's instructions (Invitrogen). Briefly, LNCaP Exo$^{Normoxic}$ or Exo$^{Hypoxic}$ (10 μg each) were mixed with equal volume of tris-glycine SDS sample buffer (2×) and incubated at room temperature for 10 minutes, and then run on 10% zymogram (gelatin) gel. The gel was then processed by incubating in zymogram renaturing buffer for 30 minutes at room temperature followed by overnight incubation in zymogram developing buffer at 37°;C and stained with Coomassie Blue. The areas of protease activity appeared as clear bands.

### Western blotting

The exosomes isolated by Exoquick™ precipitation were lysed with lysis buffer (10 mmol/L Tris-HCl, pH 7.4, 150 mmol/L NaCl, 1% Triton X-100, 1 mmol/L EDTA, 1 mmol/L EGTA, 0.3 mmol/L phenylmethylsulfonyl fluoride, 0.2 mmol/L sodium orthovanadate, 0.5% NP40, and 5 units/mL aprotinin). PC3 cells sub-cellular fractionations (membrane, cytoplasmic and nuclear) were prepared as per vendor's protocol (ThermoFisher Scientific, Rockford, IL). The protein concentration of lysates was estimated using Bio-Rad DC protein assay kit (Bio-Rad, Hercules, CA). Samples were subjected to SDS-PAGE on 8–16% tris-glycine gels and blotted onto nitrocellulose membranes. Membranes were probed with specific primary antibodies over-night at 4°C followed by peroxidase-conjugated appropriate secondary antibody for 1 h at room temperature, and visualized by ECL detection system. For certain proteins, membranes were also probed with appropriate secondary IR Dye-tagged antibodies and visualized using Odyssey infra-red imager (LI-COR Biosciences). Membranes were also

stripped and re-probed again for protein of interest. As needed, densitometry values were measured and presented below the bands as 'fold change' compared to appropriate control after loading control normalization.

## 1D SDS-PAGE and MS analysis

The purified exosomes (50 µg) were electrophoresed on a 10% 1D SDS-PAGE and the gel was stained with Coomassie brilliant blue and cut into 9 slices. Gel slices were digested using a protocol modified from Shevchenko et al.[21] Proteins were processed for protein identification by LC/MS/MS at Mass spec core facility at University of Colorado Denver. Protein data base searches of the spectra were performed with Mascot v2.2 (Matrix Science) and results were collated and protein ID's generated and validated using Protein Scape (Bruker). There were at least 2 peptides per hit, and the protein subcellular localizations and functions were determined from the Ingenuity Systems software (Redwood City, CA, USA; http://www.ingenuity.com/index.html). Pathway analysis and network constructions were assembled using the Ingenuity software.

## Statistical analysis

Statistical analysis was performed using SigmaStat 2.03 software (Jandel Scientific, San Rafael, CA). Data were analyzed using one way ANOVA (Tukey test) and a statistically significant difference was considered at $p \leq 0.05$. Statistics used for IPA (Ingenuity Pathway Analysis) can be found at the website http://www.ingenuity.com/index.html.

# RESULTS

## Characterization of LNCaP Exo$^{Normoxic}$ and Exo$^{Hypoxic}$

LNCaP Exo$^{Normoxic}$ and Exo$^{Hypoxic}$ were analyzed for particle size distribution by nanoparticle tracking analysis (NTA). As shown in Figure 1 A, the average size of Exo$^{Hypoxic}$ (average size 141 nm) was smaller than Exo$^{Normoxic}$ (average size 187 nm). NTA data also revealed that total particle concentration per ml was comparable in LNCaP Exo$^{Normoxic}$ (0.26E8 particles/mL) and Exo$^{Hypoxic}$ (0.24E8 particles/mL) after normalization with respective cell numbers. At the time of conditioned media collection for the isolation of exosomes, we observed ~50% fewer LNCaP cells under hypoxic conditions (1% $O_2$) compared to normoxic conditions (21% $O_2$), which was due to slower proliferation under hypoxic conditions. Next, we characterized LNCaP Exo$^{Normoxic}$ and Exo$^{Hypoxic}$ via electron microscopy. As shown in Figure 1B, Exo$^{Normoxic}$ and Exo$^{Hypoxic}$ were bigger than 50 nm but smaller than 100 nm. The difference between NTA and electron microscopy for exosomes size could be due to the possible aggregation of exosomes in NTA analyses.

Next, we characterized LNCaP Exo$^{Normoxic}$ and Exo$^{Hypoxic}$ for the level of proteins that are usually associated with exosomes. As shown in Figure 1C, Exo$^{Hypoxic}$ showed higher levels of tetraspanins (CD81 and CD63) compared to Exo$^{Normoxic}$. Furthermore, we also observed an increased level of HSP70 and 90 as well as Annexin II but a decreased level of Alix in Exo$^{Hypoxic}$ (Figure 1C). We did not observe any expression of endoplasmic reticulum protein Calnexin, and α-tubulin level was low in Exo$^{Normoxic}$ and Exo$^{Hypoxic}$ (Figure 1C).

## Exo$^{Hypoxic}$ enhance the invasiveness and motility of PCA cells

Earlier studies have shown that hypoxia enhances the invasiveness and motility of PCA cells [16,22]. Accordingly, next we compared the effect of LNCaP Exo$^{Normoxic}$ and Exo$^{Hypoxic}$ on the invasiveness of naïve LNCaP cells. As shown in Figure 2A, compared to Exo$^{Normoxic}$, co-culturing with Exo$^{Hypoxic}$ significantly increased the invasiveness of naïve LNCaP cells (~4-fold increase, p ≤0.05). Furthermore, we compared LNCaP Exo$^{Normoxic}$ and Exo$^{Hypoxic}$ for their effect on the motility of naïve PC3 cells in a wound healing assay. We selected PC3 cells as LNCaP cells are not suitable for this assay. As shown in Figure 2B, at 0 hr, the size of the wound was almost equal in all the groups. However, 6 hrs following incubation with or without exosomes, PC3 cells migrated and filled the wound to varying extent. The presence of Exo$^{Normoxic}$ only marginally increased the motility of PC3 cells; however, in the presence of Exo$^{Hypoxic}$ PC3 cells motility was significantly increased and wound was almost closed (Figure 2B, Left Panel). Distance traveled by cells in each case was also quantified, and we observed a significant increase in the cell migration distance in the presence of Exo$^{Hypoxic}$ (Figure 2B, Right Panel). Together, these two studies clearly established that exosomes released under hypoxia could promote the invasiveness and motility of PCA cells. This study also suggested that LNCaP Exo$^{Hypoxic}$ effect was not confined to LNCaP cells only, and LNCaP Exo$^{Hypoxic}$ could enhance the motility of PC3 cells, a cell line not of their origin.

## Exo$^{Hypoxic}$ enhance the stemness of PCA cells

Hypoxia has been associated with increased stemness in cancer cells [23]. Also, there is a great degree of overlap in cancer metastatic and stem-cell populations [24,25]. Therefore, we reasoned that besides increasing the invasiveness and motility of PCA cells, Exo$^{Hypoxic}$ could also enhance their stemness. We analyzed the effect of Exo$^{Normoxic}$ and Exo$^{Hypoxic}$ on the stemness of PCA cells in a prostasphere assay, which is considered a standard *in vitro* assay to measure the stemness of PCA cells [26,27]. Repeated treatment with LNCaP Exo$^{Hypoxic}$ enhanced prostaspheres number (1.5-fold increase compared to Exo$^{Normoxic}$, p ≤0.05) in naïve LNCaP cells (Figure 3A, Upper Panel). Similarly, PC3 Exo$^{Hypoxic}$ enhanced the prostaspheres number (1.9-fold increase compared to Exo$^{Normoxic}$, p ≤0.001) in naïve PC3 cells (Figure 3A, Bottom Panel). Together, these results suggested that Exo$^{Hypoxic}$ could enhance the stemness of PCA cells.

## Exo$^{Hypoxic}$ enhance CAF-type phenotype in prostate fibroblasts

Cancer cells secrete several growth factors and cytokines to modify fibroblasts to a CAF-type phenotype, which is known to promote angiogenesis, stemness and metastasis [5,18,19]. Since PCA exosomes secreted under hypoxic conditions could also affect the transformation of fibroblasts in the tumor microenvironment, we next examined the effect of Exo$^{Normoxic}$ and Exo$^{Hypoxic}$ on CAF-type phenotype induction in human PrSC. As shown in Figure 3B, basal α-SMA (a biomarker for the CAF phenotype) expression in PrSC was low, and in the presence of LNCaP and PC3 Exo$^{Normoxic}$, α-SMA expression was slightly enhanced. However, α-SMA expression was significantly higher and organized in PrSC in the presence of Exo$^{Hypoxic}$ from both LNCaP and PC3 cells (Figure 3B). TGF-β2 is a known

inducer of CAF phenotype [28]; therefore TGF-β2-induced PrSC (with higher expression and well organized α-SMA) were considered as a positive control in this experiment.

## Exo$^{Hypoxic}$ possess higher metalloproteinase activity and higher level of key signaling molecules

Metalloproteinases (MMPs) have been associated with angiogenesis, metastasis, and hormone-refractory progression of PCA [29]. Hypoxia has been reported to enhance MMP-2 activity in PCA cells thereby increasing their invasiveness [16]; however, MMPs activity in hypoxic PCA exosomes has not been studied. We next compared Exo$^{Normoxic}$ and Exo$^{Hypoxic}$ for their MMPs activity in zymogram assays and as shown in Figure 4A, Exo$^{Hypoxic}$ showed higher MMP-2 and MMP-9 activity compared to Exo$^{Normoxic}$.

We next compared the Exo$^{Normoxic}$ and Exo$^{Hypoxic}$ for levels of various cytokines, growth factors and signaling molecules that play important role in inter-cellular communication in the tumor microenvironment as well as PCA growth and progression [9,19,30]. As shown Figure 4B, Exo$^{Hypoxic}$ showed significantly higher levels of TGF-β2, TNF1α and IL6 compared to Exo$^{Normoxic}$. We also observed an increase in the level of TSG101 (Tumor Susceptibility Gene 101), a protein that plays a critical role in endosomal sorting and trafficking. We also detected higher Akt, ILK1 (Integrin-linked Kinase) and β-catenin levels in Exo$^{Hypoxic}$ compared to Exo$^{Normoxic}$, while no difference was observed in PKM2 level. These results suggest higher amounts of cytokines and signaling molecules in Exo$^{Hypoxic}$ compared to Exo$^{Normoxic}$.

## Exo$^{Hypoxic}$ are loaded with higher number of proteins associated with distinct signaling pathways

Next, we performed gel-based separation of Exo$^{Normoxic}$ and Exo$^{Hypoxic}$ proteins with *in situ* protease digestion of gel slices to obtain peptides for mass spectrometry mapping and *de novo* sequencing for protein identity. We identified 62 proteins in Exo$^{Normoxic}$ and 160 proteins in Exo$^{Hypoxic}$ (Figure 5A, Left Panel) and of those, 60 and 155 proteins were trackable in IPA software (Supplementary table I and table II). The proteins identified were categorized for their sub-cellular or extra-cellular localization. As shown in Figure 5A, Middle and Right Panels, Exo$^{Normoxic}$ and Exo$^{Hypoxic}$ were loaded with proteins primarily from the cytoplasm and extra-cellular space, with relatively low percentages of plasma membrane and nucleus-derived proteins. Compared to Exo$^{Normoxic}$, Exo$^{Hypoxic}$ showed a greater percentage of cytosol-derived proteins and a lesser percentage of extra-cellular-derived proteins (Figure 5A, Middle and Right Panels). However, it is important to mention here that numerous protein we categorized based upon IPA software have multiple localizations, particularly in tumors.

Using IPA software, the identified proteins were grouped into networks of associated functions and canonical pathways. In Figure 5B, we have presented the differences in the top 15 canonical pathways of Exo$^{Normoxic}$ and Exo$^{Hypoxic}$ associated proteins. The scores (−log [p value]) reflect the probabilities of such association occurring by chance, with the threshold value for significance set at 1.25. Furthermore, the top 5 networks/associated functions for Exo$^{Normoxic}$ proteins were "Dermatological Diseases and Conditions,

Developmental Disorder, Hereditary Disorder" (Score=65); Hair and Skin Development and Function, Dermatological Diseases and Conditions, Respiratory Disease" (Score=26); Cell Death and Survival, Cardiovascular System Development and Function, Cardiovascular Disease" (Score=20); Lipid Metabolism, Small Molecular Biochemistry, Cellular Movement" (Score=10); and "Cardiovascular Disease, Hematological Disease, Neurological Disease" (Score=6). The top 5 networks/associated functions for Exo$^{Hypoxic}$ proteins were "Protein Synthesis, Gene Expression, Cell Morphology" (Score=55); "Cancer, Hematological Disease, Immunological Disease" (Score=52); "Tissue Morphology, Dermatological Diseases and Conditions, Infectious Disease" (Score=51); "Neurological Disease, Psychological Disorders, Skeletal and Muscular Disorders" (Score=42); "Cancer, Reproductive System Disease, Cellular Assembly and Organization" (Score=23). Figures 5C and 5D show the "interactome" of the highest-scoring local connecting network and functional associations within these networks for Exo$^{Normoxic}$ and Exo$^{Hypoxic}$, respectively. Proteins identified in the proteomics screen are shown in black font with yellow highlights; while proteins not in the proteomics screen are shown in blue color (Figure5C and 5D). Direct interactions between identified proteins are indicated by solid lines and indirect connections are shown with broken lines. Figure 5C demonstrates the strong connectivity of the chaperone and cytoskeletal protein system with transcriptional regulators (CAND1, EEFs, and ILF2) and kinases (Akt and PGK1) in Exo$^{Normoxic}$. Similarly, Figure 5D demonstrates the strong connectivity of the chaperone and cytoskeletal protein system with transcriptional regulators (CAND1, EEFs, and HNRNPD) and kinases (JNK and CKB) in Exo$^{Hypoxic}$.

### Exo$^{Hypoxic}$ target adherens junction molecules in PCA cells

Mass spectrometry results suggested that the proteins in Exo$^{Hypoxic}$ are associated with the remodeling of the epithelial adherens junction and cytoskeleton signaling (Figure 5B). Therefore, we examined the effect of LNCaP Exo$^{Hypoxic}$ on the adherens junction proteins in naïve PC3 cells. It is important to mention here that adherens junction proteins at the membrane (E-cadherin and catenins) maintain cell-cell contact and inhibit invasiveness/ motility of cells. Our results showed that compared to Exo$^{Normoxic}$, Exo$^{Hypoxic}$ treatment decreased E-cadherin expression in the membrane fraction of PC3 cells (Figure 6A). We did not observe E-cadherin expression in the cytoplasmic fraction confirming the purity of membrane fractions. Furthermore, there was an increase in the nuclear and cytoplasmic β-catenin level in PC3 cells in the presence of Exo$^{Hypoxic}$ compared to Exo$^{Normoxic}$ but there was no significant change in the β-catenin level in the membrane fraction. PARP and α-tubulin blots confirmed equal protein loading in nuclear and cytoplasmic fractions respectively.

## DISCUSSION

As the primary tumor mass grows, tumor cells at the core get limited supply of oxygen and nutrients and are immersed in a stew of metabolic waste, acidic pH and necrotic cells, a physiological condition termed as 'hypoxia'. To overcome these hostile conditions, tumor cells activate transcriptional machinery leading to neo-angiogenesis, altered anaerobic metabolism and increased invasiveness [15,23]. However, the precise mechanism through

which hypoxic tumor cells at the core of a tumor transmit signals to cells at the periphery ("the invasive front") for migration remains unknown. We hypothesized that hypoxic prostate tumor cells secrete 'exosomes', small vesicles of approximately 30–100 nM diameter carrying proteins, mRNA and miRNAs, which fuse with the surrounding and/or distant tumor cells and microenvironment cells (such as fibroblasts) and significantly enhance PCA cells invasiveness and metastasis. Results from present study support this hypothesis, and for the first time we present that 1) exosomes secreted by PCA cells under hypoxia are loaded with significantly higher number of proteins; 2) hypoxic PCA exosomes could target adherens junction molecules; and 3) hypoxic PCA exosomes could significantly enhance the motility, invasiveness and stemness of naïve PCA cells.

Recent studies suggested that hypoxic conditions could promote metastasis through re-modeling and preparing distant pre-metastatic niches [31–33]. In this regard, Erler et al [31] reported that lysyl oxidase (LOX) secreted by hypoxic breast tumor cells plays an important role in the enhancement of metastatic tumor growth through promoting the recruitment of bone marrow cells at pre-metastatic niches. Similarly, Wong et al [32] reported that HIF-1α is a critical regulator of breast cancer metastatic niche formation through the induction of LOX family members. Hypoxic conditions also promote the release of exosomes by breast cancer cells in a HIF-1α dependent manner [34]. Thus, there is a strong possibility that under hypoxic conditions, signals for enhanced invasiveness are transferred through exosomes both locally as well as to distant pre-metastatic niches. Peinado et al [13] recently confirmed that exosomes play an important role in pre-metastatic niches formation even though this study did not analyze the hypoxia status of the primary melanoma tumors. Results from the present study showed a higher number of proteins loaded in hypoxic exosomes even though we did not observe any additional increases in exosomes number under hypoxic conditions. Importantly, several of the Exo$^{Hypoxic}$ proteins (e.g. TGF-β, IL6, TNF1α, MMPs etc) have been implicated in promoting pre-metastatic niche formation as well as inducing stemness and EMT in cancer cells [9,19,23,30].

It is known that metastasis by PCA cells involves multiple steps, and among these events, EMT has for some time been considered an absolute and indispensable element for metastasis [35,36]. During EMT, cancer cells shed their epithelial characteristics, detach from epithelial sheets and undergo cytoskeletal alterations towards a more 'mesenchymal phenotype' and acquire a high degree of motility and invasiveness [35,36]. The molecular basis of EMT is very complex and involves several interconnected pathways that down-regulate the expression of adherens junction molecule E-cadherin, which is well-known for regulating cell-to-cell contact, cell shape and polarity [35,37]. E-cadherin connects adjacent cells through homophilic interactions and is also linked to the cytoskeleton though multi-catenin complex attached to their cytoplasmic tails [38,39]. In this complex, β-catenin and p120 are directly associated with E-cadherin, while α-catenin is the link between β-catenin and the actin microfilament network of the cytoskeleton [38,39]. Loss of E-cadherin results in loss of cell to cell contact, disruption of E-cadherin-catenin complex, abnormal activation of β-catenin signaling and cellular cytoskeletal alterations [35,40]. Overall, these changes are essential for cells to lose their epithelial polarity and to acquire an invasive phenotype [35,36]. In primary PCA, reduced E-cadherin expression and nuclear β-catenin expression have been correlated with increased tumor grade, metastasis and a poor prognosis [41–43].

Interestingly, Gupta et al [44] have shown in breast cancer cells that E-cadherin down-regulation not only induces EMT and invasiveness but also promotes a 'stem-like cell population'. In the present study, MS and IPA analyses showed that Exo$^{Hypoxic}$ proteins are strongly involved in canonical pathways linked with epithelial adherens junctions and cytoskeleton remodeling. Furthermore, we observed that Exo$^{Hypoxic}$ promoted E-cadherin loss in PC3 cells along with an increase in cytoplasmic and nuclear β-catenin expression. Based upon known literature, these changes could be responsible for the observed increase in the invasiveness, motility and stemness of PCA cells by Exo$^{Hypoxic}$; however, we did not analyze the mechanisms through which Exo$^{Hypoxic}$ targets elements of the adherens junction, whether it is through the MMP -mediated cleavage of E-cadherin or through the protein and miRNA content released by Exo$^{Hypoxic}$ in naïve PCA cells (as shown in the model described in Figure 6B).

Overall, the present study provides new evidence that under hypoxic conditions, the aggressiveness of PCA cells could be increased through exosomes. Further studies are warranted to confirm these results in *in vivo* settings, and to understand the role of specific proteins and miRNAs loaded in hypoxic exosomes. Also, we need to better understand the alterations in exosome production and release machinery under hypoxic conditions, which would be helpful to target the production of exosomes and to prevent metastatic onset in PCA cells.

## Supplementary Material

Refer to Web version on PubMed Central for supplementary material.

## ACKNOWLEDGEMENT

## List of Abbreviations

| | |
|---|---|
| **ANOVA** | Analysis of variance |
| **α-SMA** | Alpha-smooth muscle actin |
| **CAF** | Cancer-associated fibroblast |
| **DAPI** | 4, 6-diamidino-2-phenylindole |
| **ECL** | Enhanced chemiluminescence |
| **EMT** | Epithelial to mesenchymal transition |
| **FBS** | Fetal bovine serum |
| **HRP** | Horseradish peroxidase |
| **IL6** | Interleukin 6 |

| **LOX** | Lysyl oxidase |
|---|---|
| **MMP** | Matrix metalloproteinase |
| **MS** | Mass spectrometry |
| **NTA** | Nanoparticle tracking analysis |
| **PAGE** | Polyacrylamide gel electrophoresis |
| **PCA** | Prostate cancer |
| **PKM2** | Pyruvate kinase M2 |
| **PrSC** | Prostate stromal cells |
| **SCGM** | Stromal cell growth medium |
| **SDS** | Sodium dodecyl sulfate |
| **TGF-β2** | Transforming growth factor beta 2 |
| **TNF1α** | Tumor necrosis factor 1 alpha |

## References

1. Siegel R, Naishadham D, Jemal A. Cancer statistics, 2013. CA Cancer J Clin. 2013; 63:11–30. [PubMed: 23335087]

2. Kingsley LA, Fournier PG, Chirgwin JM, Guise TA. Molecular biology of bone metastasis. Mol Cancer Ther. 2007; 6:2609–2617. [PubMed: 17938257]

3. Tantivejkul K, Kalikin LM, Pienta KJ. Dynamic process of prostate cancer metastasis to bone. J Cell Biochem. 2004; 91:706–717. [PubMed: 14991762]

4. Hadaschik BA, Gleave ME. Therapeutic options for hormone-refractory prostate cancer in 2007. Urol Oncol. 2007; 25:413–419. [PubMed: 17826663]

5. Albini A, Sporn MB. The tumour microenvironment as a target for chemoprevention. Nat Rev Cancer. 2007; 7:139–147. [PubMed: 17218951]

6. Joyce JA. Therapeutic targeting of the tumor microenvironment. Cancer Cell. 2005; 7:513–520. [PubMed: 15950901]

7. Deep G, Agarwal R. Targeting Tumor Micro environment with Silibinin: Promise and Potential for a Translational Cancer Chemopreventive Strategy. Curr Cancer Drug Targets. 2013

8. Azmi AS, Bao B, Sarkar FH. Exosomes in cancer development, metastasis, and drug resistance: a comprehensive review. Cancer Metastasis Rev. 2013

9. Sceneay J, Smyth MJ, Moller A. The pre-metastatic niche: finding common ground. Cancer Metastasis Rev. 2013

10. Keller S, Sanderson MP, Stoeck A, Altevogt P. Exosomes: from biogenesis and secretion to biological function. Immunol Lett. 2006; 107:102–108. [PubMed: 17067686]

11. Epple LM, Griffiths SG, Dechkovskaia AM, et al. Medulloblastoma exosome proteomics yield functional roles for extracellular vesicles. PLoS One. 2012; 7:e42064. [PubMed: 22848702]

12. Hosseini-Beheshti E, Pham S, Adomat H, Li N, Tomlinson Guns ES. Exosomes as biomarker enriched microvesicles: characterization of exosomal proteins derived from a panel of prostate cell lines with distinct AR phenotypes. Mol Cell Proteomics. 2012; 11:863–885. [PubMed: 22723089]

13. Peinado H, Aleckovic M, Lavotshkin S, et al. Melanoma exosomes educate bone marrow progenitor cells toward a pro-metastatic phenotype through MET. Nat Med. 2012; 18:883–891. [PubMed: 22635005]

14. Bao B, Ahmad A, Kong D, et al. Hypoxia induced aggressiveness of prostate cancer cells is linked with deregulated expression of VEGF, IL-6 and miRNAs that are attenuated by CDF. PLoS One. 2012; 7:e43726. [PubMed: 22952749]

15. Tatum JL, Kelloff GJ, Gillies RJ, et al. Hypoxia: importance in tumor biology, noninvasive measurement by imaging, and value of its measurement in the management of cancer therapy. Int J Radiat Biol. 2006; 82:699–757. [PubMed: 17118889]

16. Dai Y, Bae K, Siemann DW. Impact of hypoxia on the metastatic potential of human prostate cancer cells. Int J Radiat Oncol Biol Phys. 2011; 81:521–528. [PubMed: 21640519]

17. Butterworth KT, McCarthy HO, Devlin A, et al. Hypoxia selects for androgen independent LNCaP cells with a more malignant geno- and phenotype. Int J Cancer. 2008; 123:760–768. [PubMed: 18512241]

18. Fiaschi T, Giannoni E, Taddei ML, et al. Carbonic anhydrase IX from cancer-associated fibroblasts drives epithelial-mesenchymal transition in prostate carcinoma cells. Cell Cycle. 2013; 12:1791–1801. [PubMed: 23656776]

19. Giannoni E, Bianchini F, Masieri L, et al. Reciprocal activation of prostate cancer cells and cancer-associated fibroblasts stimulates epithelial-mesenchymal transition and cancer stemness. Cancer Res. 2010; 70:6945–6956. [PubMed: 20699369]

20. Deep G, Gangar SC, Agarwal C, Agarwal R. Role of E-cadherin in antimigratory and antiinvasive efficacy of silibinin in prostate cancer cells. Cancer Prev Res (Phila). 2011; 4:1222–1232. [PubMed: 21546539]

21. Shevchenko A. Evaluation of the efficiency of in-gel digestion of proteins by peptide isotopic labeling and MALDI mass spectrometry. Anal Biochem. 2001; 296:279–283. [PubMed: 11554724]

22. Luo Y, He DL, Ning L, Shen SL, Li L, Li X. Hypoxia-inducible factor-1alpha induces the epithelial-mesenchymal transition of human prostatecancer cells. Chinese Medical Journal. 2006; 119:713–718. [PubMed: 16701010]

23. Mimeault M, Batra SK. Hypoxia-inducing factors as master regulators of stemness properties and altered metabolism of cancer- and metastasis-initiating cells. J Cell Mol Med. 2013; 17:30–54. [PubMed: 23301832]

24. Mani SA, Guo W, Liao MJ, et al. The epithelial-mesenchymal transition generates cells with properties of stem cells. Cell. 2008; 133:704–715. [PubMed: 18485877]

25. Polyak K, Weinberg RA. Transitions between epithelial and mesenchymal states: acquisition of malignant and stem cell traits. Nat Rev Cancer. 2009; 9:265–273. [PubMed: 19262571]

26. Bisson I, Prowse DM. WNT signaling regulates self-renewal and differentiation of prostate cancer cells with stem cell characteristics. Cell Res. 2009; 19:683–697. [PubMed: 19365403]

27. Guzman-Ramirez N, Voller M, Wetterwald A, et al. In vitro propagation and characterization of neoplastic stem/progenitor-like cells from human prostate cancer tissue. Prostate. 2009; 69:1683–1693. [PubMed: 19644960]

28. Kojima Y, Acar A, Eaton EN, et al. Autocrine TGF-beta and stromal cell-derived factor-1 (SDF-1) signaling drives the evolution of tumor-promoting mammary stromal myofibroblasts. Proc Natl Acad Sci U S A. 2010; 107:20009–20014. [PubMed: 21041659]

29. Miyamoto H, Altuwaijri S, Cai Y, Messing EM, Chang C. Inhibition of the Akt, cyclooxygenase-2, and matrix metalloproteinase-9 pathways in combination with androgen deprivation therapy: potential therapeutic approaches for prostate cancer. Mol Carcinog. 2005; 44:1–10. [PubMed: 16044418]

30. Meads MB, Hazlehurst LA, Dalton WS. The bone marrow microenvironment as a tumor sanctuary and contributor to drug resistance. Clin Cancer Res. 2008; 14:2519–2526. [PubMed: 18451212]

31. Erler JT, Bennewith KL, Cox TR, et al. Hypoxia-induced lysyl oxidase is a critical mediator of bone marrow cell recruitment to form the premetastatic niche. Cancer Cell. 2009; 15:35–44. [PubMed: 19111879]

32. Wong CC, Gilkes DM, Zhang H, et al. Hypoxia-inducible factor 1 is a master regulator of breast cancer metastatic niche formation. Proc Natl Acad Sci U S A. 2011; 108:16369–16374. [PubMed: 21911388]

33. Sceneay J, Chow MT, Chen A, et al. Primary tumor hypoxia recruits CD11b+/Ly6Cmed/Ly6G+ immune suppressor cells and compromises NK cell cytotoxicity in the premetastatic niche. Cancer Res. 2012; 72:3906–3911. [PubMed: 22751463]

34. King HW, Michael MZ, Gleadle JM. Hypoxic enhancement of exosome release by breast cancer cells. BMC Cancer. 2012; 12:421. [PubMed: 22998595]

35. Guarino M, Rubino B, Ballabio G. The role of epithelial-mesenchymal transition in cancer pathology. Pathology. 2007; 39:305–318. [PubMed: 17558857]

36. Christiansen JJ, Rajasekaran AK. Reassessing epithelial to mesenchymal transition as a prerequisite for carcinoma invasion and metastasis. Cancer Res. 2006; 66:8319–8326. [PubMed: 16951136]

37. Baranwal S, Alahari SK. Molecular mechanisms controlling E-cadherin expression in breast cancer. Biochem Biophys Res Commun. 2009; 384:6–11. [PubMed: 19379710]

38. Inge LJ, Rajasekaran SA, Wolle D, et al. alpha-Catenin overrides Src-dependent activation of beta-catenin oncogenic signaling. Mol Cancer Ther. 2008; 7:1386–1397. [PubMed: 18566211]

39. Ebnet K. Organization of multiprotein complexes at cell-cell junctions. Histochem Cell Biol. 2008; 130:1–20. [PubMed: 18365233]

40. Onder TT, Gupta PB, Mani SA, Yang J, Lander ES, Weinberg RA. Loss of E-cadherin promotes metastasis via multiple downstream transcriptional pathways. Cancer Res. 2008; 68:3645–3654. [PubMed: 18483246]

41. Umbas R, Isaacs WB, Bringuier PP, et al. Decreased E-cadherin expression is associated with poor prognosis in patients with prostate cancer. Cancer Res. 1994; 54:3929–3933. [PubMed: 7518346]

42. Umbas R, Schalken JA, Aalders TW, et al. Expression of the cellular adhesion molecule E-cadherin is reduced or absent in high-grade prostate cancer. Cancer Res. 1992; 52:5104–5109. [PubMed: 1516067]

43. Cheng L, Nagabhushan M, Pretlow TP, Amini SB, Pretlow TG. Expression of E-cadherin in primary and metastatic prostate cancer. Am J Pathol. 1996; 148:1375–1380. [PubMed: 8623909]

44. Gupta PB, Onder TT, Jiang G, et al. Identification of selective inhibitors of cancer stem cells by high-throughput screening. Cell. 2009; 138:645–659. [PubMed: 19682730]
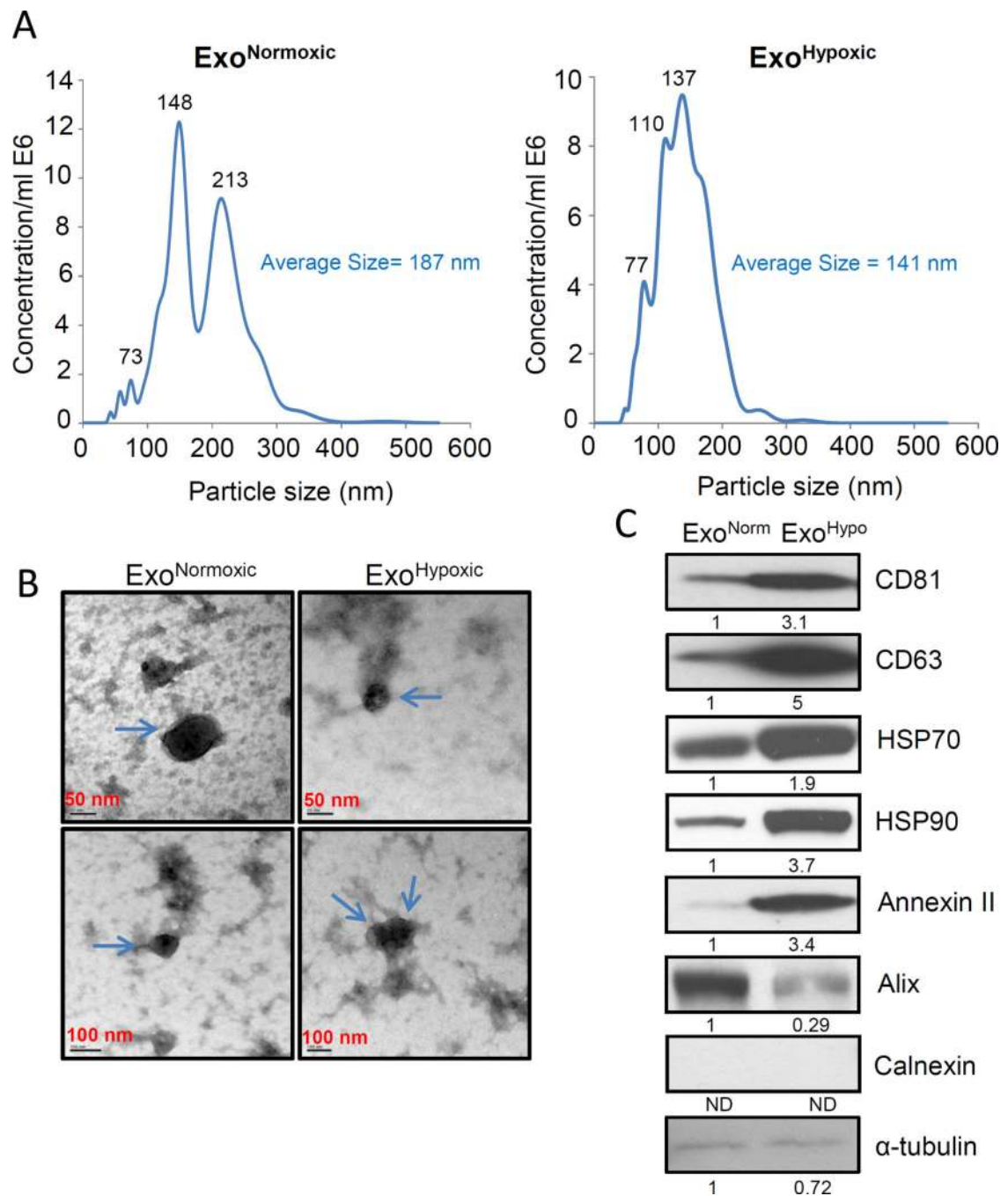
**Figure 1. Characterization of Exo$^{Normoxic}$ and Exo$^{Hypoxic}$**

(**A**) Exo$^{Normoxic}$ and Exo$^{Hypoxic}$ were analyzed for particle size and concentration by NTA using a NanoSight device. Representative particle distributions for Exo$^{Normoxic}$ (Left Panel) and Exo$^{Hypoxic}$ (Right Panel) are presented. (**B**) Exo$^{Normoxic}$ and Exo$^{Hypoxic}$ were analyzed by electron microscopy as detailed in the 'Materials and Methods' and representative photomicrographs are shown (arrow points to exosomes). (**C**) Exo$^{Normoxic}$ and Exo$^{Hypoxic}$ collected through precipitation method were lysed and protein expressions of CD81, CD63, HSP70, HSP90, annexin II, Alix, Calnexin, and α-tubulin were analyzed by Western

blotting after equal amount of protein loading. Mean densitometry values are presented below the bands (ND: Not detectable). These results were similar in at least two independent experiments.
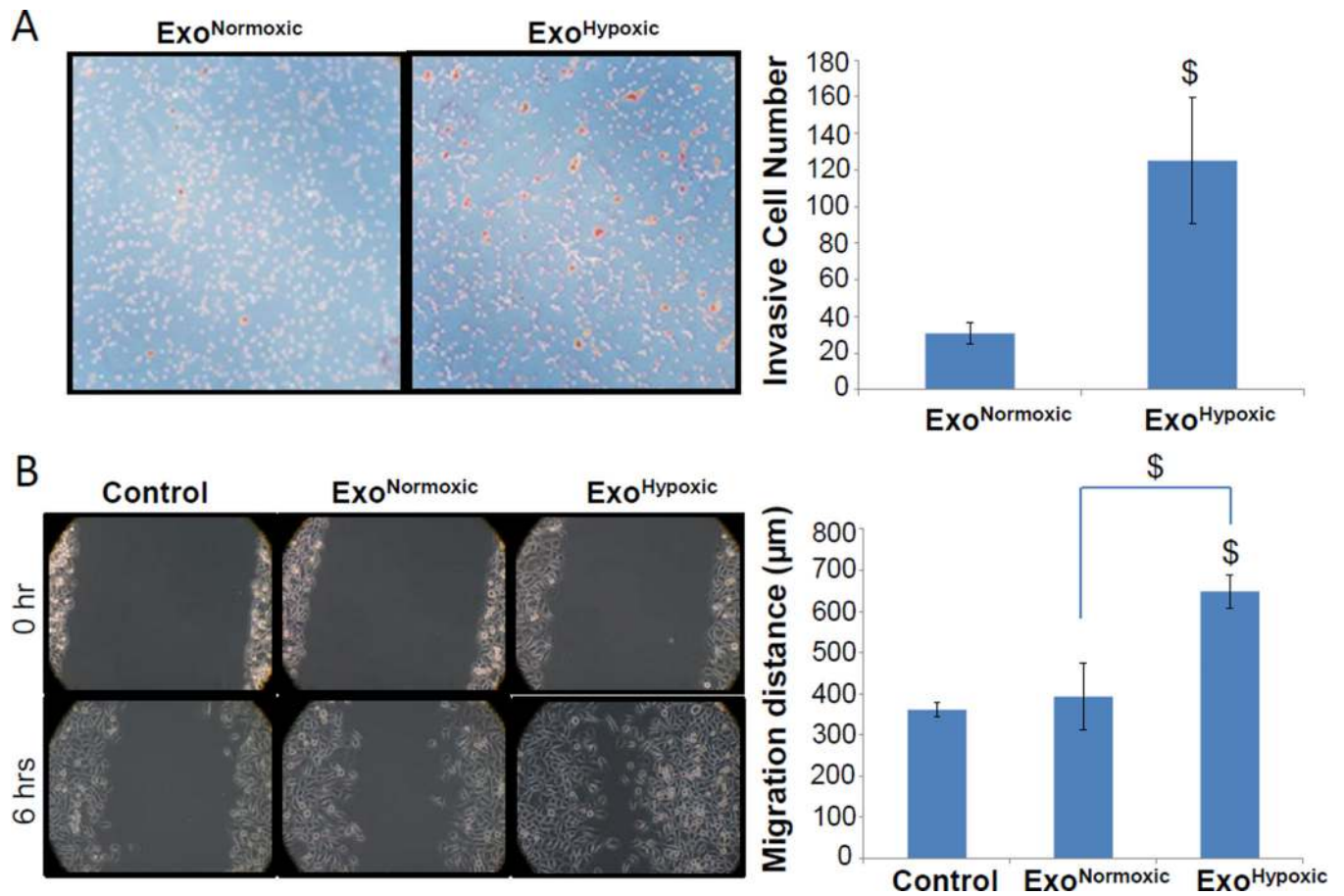
**Figure 2. Exo<sup>Hypoxic</sup> promote invasiveness and motility in PCA cells**

**(A)** Effects of LNCaP Exo$^{Normoxic}$ and Exo$^{Hypoxic}$ were analyzed on the invasiveness of naïve LNCaP cells using invasion chambers. Cell invasion data shown are means±SEM of four samples. **(B)** Effects of LNCaP Exo$^{Normoxic}$ and Exo$^{Hypoxic}$ were analyzed on the migratory potential of PC3 cells through wound healing assays. Representative photomicrographs of initial (at 0 hr) and final wounds (after 6 hrs) are shown at 100× magnification. Cell migration distance data shown is mean±SEM of three samples. $, p ≤0.05
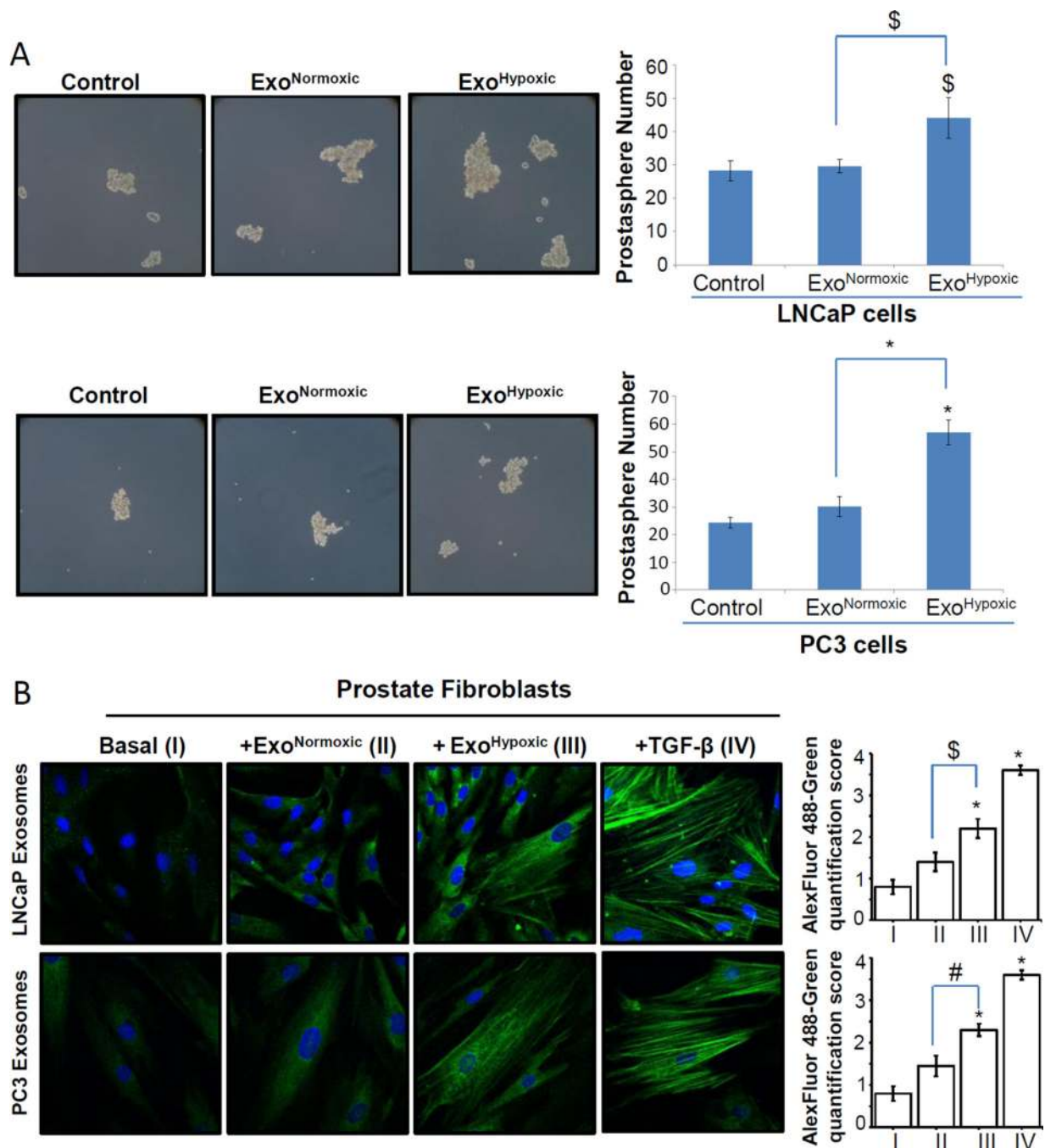
**Figure 3. Exo^Hypoxic promote stemness in PCA cells and CAF-phenotype in prostate fibroblasts**
(**A**) Effects of Exo^Normoxic and Exo^Hypoxic were analyzed on the stemness of naïve LNCaP (upper panel) and PC3 cells (Bottom Panel) following procedures detailed in the 'Materials and Methods'. Prostasphere formation was analyzed after 5–6 days and representative pictures (prostaspheres marked by arrows) are shown at 100× magnification. Prostasphere data shown is mean±SEM of six samples. (**B**) Human prostate stromal cells (PrSC) were cultured in the presence of Exo^Normoxic and Exo^Hypoxic from LNCaP (Upper Panel) and PC3 cells (Bottom Panel), and α-SMA expression was analyzed by confocal microscopy.

Representative images from three independent experiments are shown at 1000× magnification, where Alexa Fluor 488-green is for α-SMA while DAPI-blue stains nuclei. PrSC without exosomes represent the basal expression of α-SMA, while PrSC treated with TGF-β2 served as a positive control. Alexa-Fluor 488 -green quantification data shown is mean±SEM of twenty images from three independent experiments. \$, $p \leq 0.05$; #, $p \leq 0.01$; *, $p \leq 0.001$
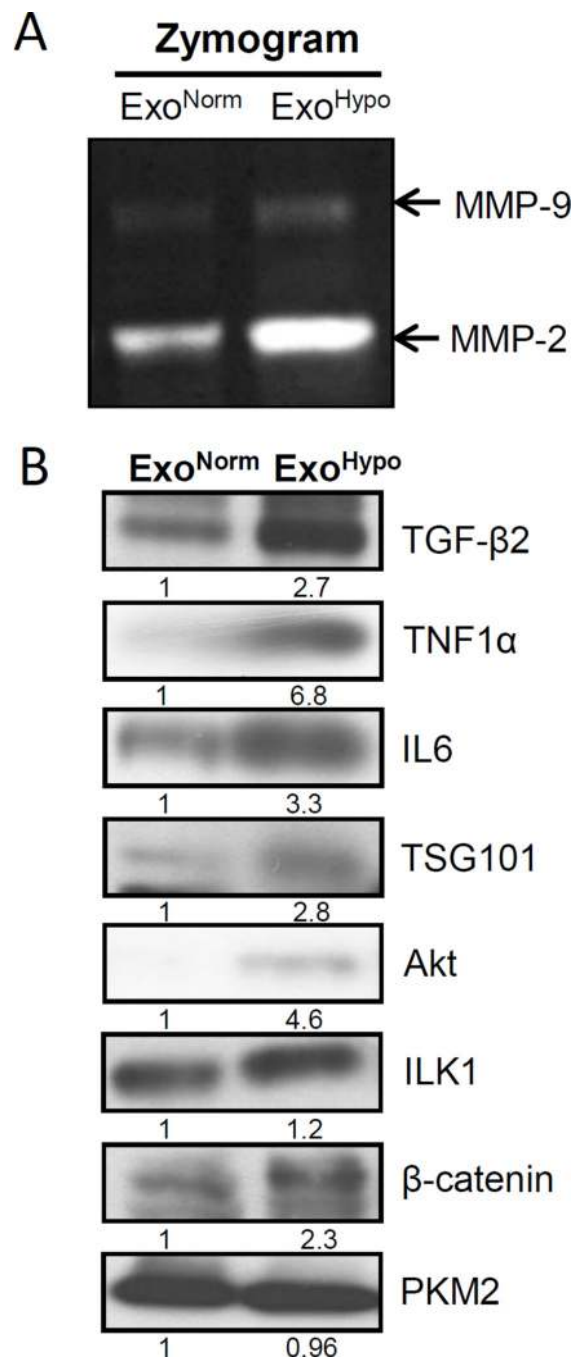
**Figure 4. Exo<sup>Hypoxic</sup> exhibit enhanced metalloproteinases (MMPs) activity and expression of signaling molecules**

(**A**) MMP2 and 9 activities in Exo$^{Normoxic}$ and Exo$^{Hypoxic}$ were analyzed by zymogram assay. Gels were scanned and representative pictures are shown. (**B**) Exo$^{Normoxic}$ and Exo$^{Hypoxic}$ collected through precipitation method were lysed and protein expression of TGF-β2, TNF1α, IL6, TSG101, Akt, ILK1, β-catenin, and PKM2 was analyzed by Western blotting. Mean densitometry values are presented below the bands. These results were similar in at least two independent experiments.
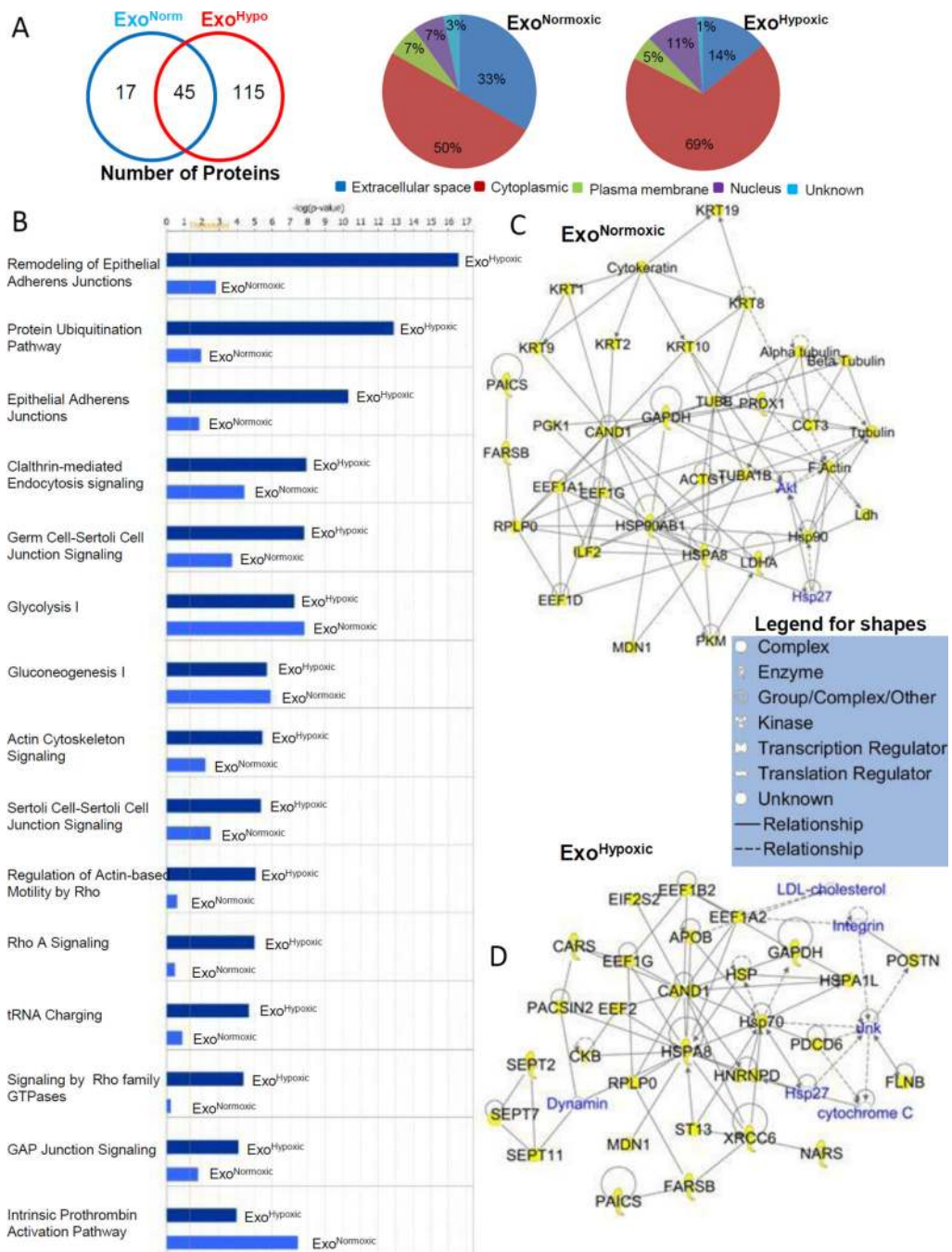
**Figure 5. Characterization of Exo^Normoxic and Exo^Hypoxic proteins by mass spectrometry**
(**A**) Total proteins (both distinct and overlapping) present in Exo^Normoxic and Exo^Hypoxic are presented in a Venn diagram (Left Panel). Proteins were characterized using Ingenuity IPA software, and proteins subcellular (or extracellular) localization is presented in pie diagrams (Middle and Right Panel). (**B**) Exo^Normoxic and Exo^Hypoxic total protein data were compared using Ingenuity IPA software. Comparisons of the Top 15 canonical pathways are shown. Scores (total number of proteins in the sample versus total number of known proteins of that pathway) are plotted as –log value, which is derived from a p-value and indicates the

likelihood of the Focus Proteins in a network being found together due to random chance. Threshold value is set at 1.25. **(C–D)** Exo$^{Normoxic}$ and Exo$^{Hypoxic}$ proteins clustered within the Top Networks/Associated Functions as derived from IPA algorithms are shown as members of the "interactomes". Protein shapes are indicative of function and that legend is shown.
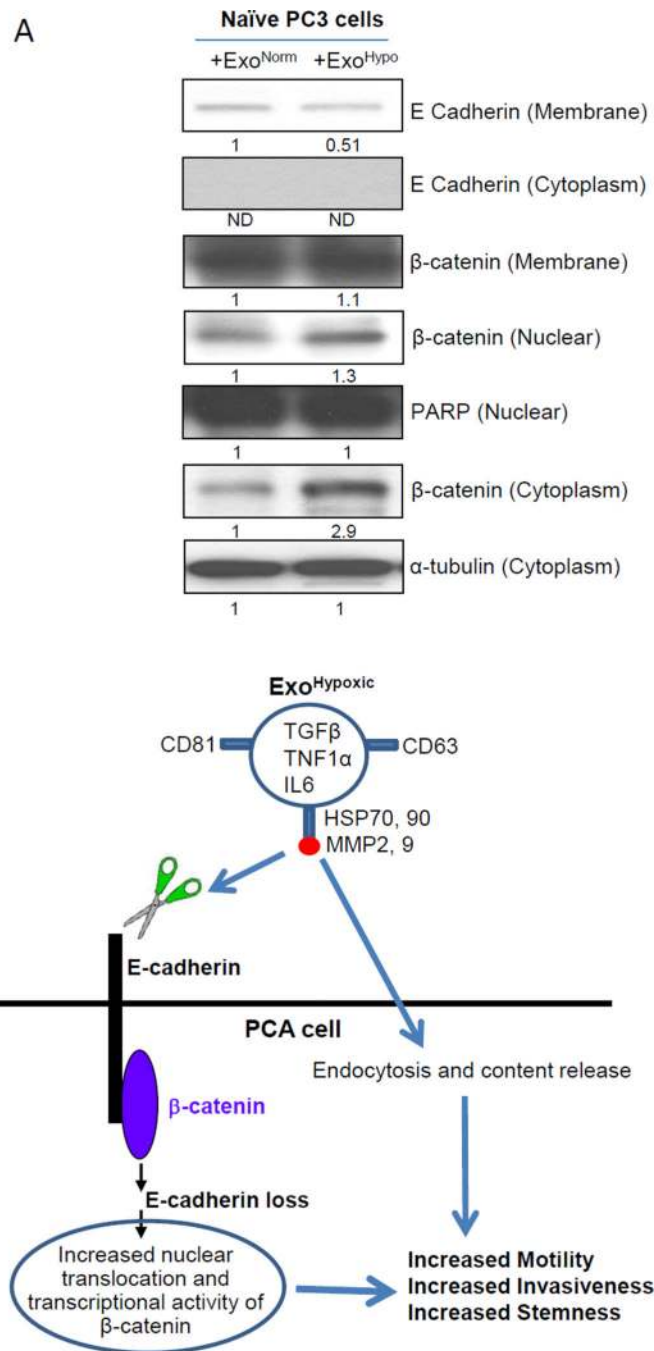
**Figure 6. Exo<sup>Hypoxic</sup> target adheren junction proteins in PC3 cells**

(**A**) Naïve PC3 cells were cultured for 24 hrs in 0.5% FBS condition, and thereafter treated with LNCaP Exo<sup>Normoxic</sup> and Exo<sup>Hypoxic</sup> (100 μg/day each) for 3 days. Thereafter, expression of adherens junction molecules E-cadherin and β-catenin was analyzed in various sub-cellular fractions. PARP and α-tubulin blots are presented as loading control for nuclear and cytoplasmic fractions respectively. Mean densitometry values are presented below the bands. ND: Not detectable (**B**) Proposed mechanism for increased motility, invasiveness and stemness of PCA cells by exosomes secreted under hypoxic conditions. Exo<sup>Hypoxic</sup> could

disrupt adheren junctions by promoting E-cadherin degradation as well as nuclear translocation of β-catenin, thereby enhancing the motility, invasiveness and stemness of PCA cells.